Acta Cryst E CRYSTALLOGRAPHIC COMMUNICATIONS

ISSN 2056-9890

Synthesis and structure of a tetrahedral homoleptic Cu^{I} complex with xylyl isocyanide

A. M. Buddhika Chandima,[a] Stanislav Groysman[a]* and Cassandra L. Ward[b]*

[a]Department of Chemistry, Wayne State University, 5101 Cass Avenue, Detroit, Michigan 48202, USA, and [b]Lumigen Instrument Center, Wayne State University, 5101 Cass Avenue, Detroit, Michigan 48202, USA. *Correspondence e-mail: groysman@wayne.edu, ward@wayne.edu

Received 14 October 2025
Accepted 5 November 2025

Edited by L. Suescun, Universidad de la República, Uruguay

Keywords: copper(I) isocyanide; Mo/Cu–CO dehydrogenase; crystal structure; π–π stacking; Hirshfeld surface analysis.

CCDC reference: 2500684

Supporting information: this article has supporting information at journals.iucr.org/e

Treatment of the Cu^{I} precursor $[Cu(NCMe)_4]PF_6$ with excess (10 equivalents) of relatively bulky xylyl isocyanide formed a tetra(isocyanide) complex, namely, tetrakis(2,6-dimethylphenylisocyanide)copper(I) hexafluorophosphate, $[Cu(C_9H_9N)_4]PF_6$ or $[Cu(CNXyl)_4]PF_6$, in good yield. This is in contrast to the previously reported reactions of Cu^{I} precursors with approximately three equivalents of xylyl isocyanide, which led selectively to the formation of tris-(isocyanide) complexes. The copper atom lies on a twofold axis and P atom on an inversion centre. The complex was characterized by X-ray crystallography, IR spectroscopy, and $^{1}H/^{13}C\{^{1}H\}$ NMR spectroscopy. In the crystal structure, each individual $[Cu(CNXyl)_4]^{+}$ molecule demonstrates two pairs of coplanar xylyl isocyanide ligands. This arrangement leads to intermolecular π-stacking interactions between nearby complex molecules.

1. Chemical context

There is a significant interest in Cu^{I} complexes in poly-(isocyanide) ligands environments. Tris(isocyanide) Cu^{I} complexes have been shown to serve as versatile platforms for catalysis and small-molecule activation (Melekhova *et al.*, 2015; Ferraro *et al.*, 2021, 2023; Kinzhalov *et al.*, 2022; Kinzhalov *et al.*, 2023), whereas tetra(isocyanide) Cu^{I} complexes serve as nodal points in photoactive materials and MOFs, or function as transmetallation reagents (Bartholomew *et al.*, 2022; Balto *et al.*, 2021; Claude *et al.*, 2023; Ruiz & Mateo, 2022). A survey of the Cambridge Structural Database appears to demonstrate a general trend in which non-bulky aryl isocyanide ligands (lacking ortho substituents) form tetrakis(isocyanide) Cu^{I} complexes (Bartholomew *et al.*, 2022; Balto *et al.*, 2021; Claude *et al.*, 2023; Ruiz & Mateo, 2022; Perrine *et al.*, 2010), whereas somewhat bulkier *ortho*-disubstituted xylyl (2,6-dimethylphenyl) isocyanide (CNXyl) forms tris(isocyanide) Cu^{I} complexes adopting a trigonal-planar or trigonal-monopyramidal geometry (Melekhova *et al.*, 2015; Ferraro *et al.*, 2021, 2023; Kinzhalov *et al.*, 2022, 2023). Notably, bulkier $CN(2,6\text{-}Mes_2C_6H_3)$ (Mes = mesityl, 2,4,6-$Me_3C_6H_2$) was shown to demonstrate a preference for tris-(isocyanide) ligation and a trigonal-planar geometry [in $Cu(CNAr)_3(THF)$], although a closely related *para*-functionalized $CN(2,6\text{-}Mes)_2C_4H_3\text{-}4\text{-}C_6H_4CO_2H$ was also capable of forming a tetra(isocyanide) Cu^{I} complex under certain conditions (Balto *et al.*, 2021; Fox *et al.*, 2008). We also note that Walton, Edwards, and coworkers reported spectroscopic characterization of a tetrakis(xylylisocyanide) Cu^{I} complex; however, these findings were not supported structurally (Bell *et al.*, 1985). We are pursuing Cu^{I} isocyanide chemistry as part of an investigation into the functional models of Mo–Cu CO

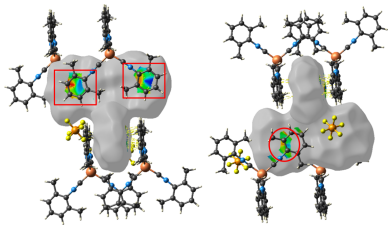

dehydrogenase (Dobbek *et al.*, 2002; Kaluarachchige Don *et al.*, 2021, 2023*a*,*b*, 2024; Hollingsworth *et al.*, 2018; Chandima *et al.*, 2025). As part of this project, we became interested in the synthesis of homoleptic Cu^{I} precursors with relatively bulky isocyanide ligand CNXyl (Xyl = 2,6-dimethylphenyl). Herein we demonstrate that the reaction of Cu^{I} precursor with excess CNXyl invariably leads to the formation of $[Cu(CNXyl)_4]^+$. The structural and spectroscopic characterization of this complex are reported.

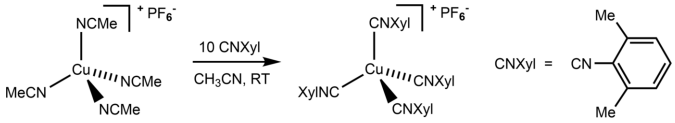

$[Cu(CNXyl)_4]PF_6$ is formed by the reaction between $[Cu(NCMe)_4]PF_6$ with excess (10 equivalents) of xylyl isocyanide, followed by recrystallization from dichloromethane/ether solution. $[Cu(CNXyl)_4]PF_6$ was characterized by ^1H and ^{13}C $\{^1H\}$ NMR spectroscopy, FT-IR spectroscopy, and X-ray crystallography. The spectroscopic data are consistent with the single species in solution. ^1H NMR demonstrates three resonances in a 1:2:6 ratio: triplet for the single proton in the *para* position of the xylyl ligand, doublet for the two *meta* protons, and a singlet for the two methyl groups. The ^{13}C $\{^1H\}$ NMR spectrum (CD_2Cl_2) demonstrates four aromatic signals, an aliphatic signal, and a signal at 146.47 ppm suggestive of coordinated isocyanide (Ferraro *et al.*, 2021). IR (ATR) features a signal at 2153 cm^{-1} consistent with the C≡N(Ar) coordinated to a non π-basic Cu^{I} (Ferraro *et al.*, 2021; Chandima *et al.*, 2025; Kaluarachchige Don *et al.*, 2021, 2023*a*,*b*, 2024; Hollingsworth *et al.*, 2018); this signal appears at slightly lower frequency compared with the previously reported $[Cu(CNXyl)_3]^+$ (υ_{CN} = 2170 cm^{-1}). No signals consistent with the presence of free isocyanide, or other metal species were observed by NMR or IR.

Table 1
Selected geometric parameters (Å, °).

Cu1—C1	1.9605 (18)	N1—C1	1.152 (2)
Cu1—C2	1.9610 (18)	N2—C2	1.154 (2)
C1—Cu1—C1^{i}	112.99 (11)	C1—N1—C3	176.48 (18)
C1—Cu1—C2	111.56 (7)	C2—N2—C11	177.1 (2)
C1—Cu1—C2^{i}	105.02 (8)	N1—C1—Cu1	174.35 (17)
C2^{i}—Cu1—C2	110.85 (11)	N2—C2—Cu1	176.58 (16)

Symmetry code: (i) $-x+1, y, -z+\frac{1}{2}$.

2. Structural commentary

The crystals of $[Cu(CNXyl)_4]PF_6$ were obtained by vapour diffusion using CH_2Cl_2/ether solvent mixture at 238 K. The compound crystallizes in the *C*2/*c* space group. The structure is presented in Fig. 1 and selected bond distances and angles are presented in Table 1. The molecule occupies a special position (twofold rotation), with only half of the complex (and anion positioned on an inversion center) constituting an asymmetric unit. The metal center exhibits a slightly distorted tetrahedral geometry, with C—Cu—C angles ranging between 105.02 (8) and 112.99 (11)°. Cu—C bonds of 1.9605 (18) and 1.9610 (18) Å are significantly longer than the Cu—C bonds in the previously described trigonal complex $[Cu(CNXyl)_3]^+$ [1.908 (2)–1.919 (1) Å; Ferraro *et al.*, 2021]. Interestingly, pairs of isocyanides within the complex (C1N1Xyl and C2′N2′Xyl, C1′N1′Xyl and C2N2Xyl) exhibit coplanar arrangements of

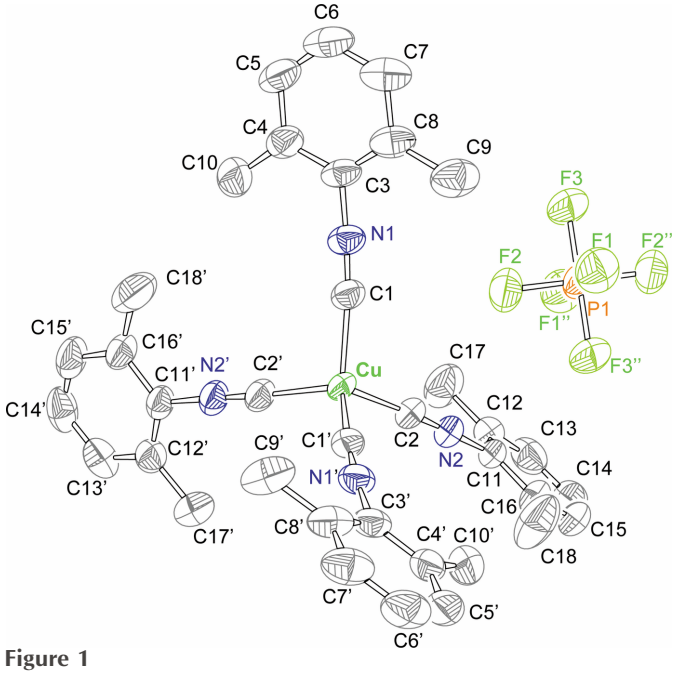

Figure 1
The structure of $[Cu(CNXyl)]_4(PF_6)$ with 50% probability ellipsoids. [Symmetry codes: (′) $-x+1, y, -z+\frac{1}{2}$; (″) $-x+\frac{1}{2}, -y+\frac{3}{2}, -z+1$.]

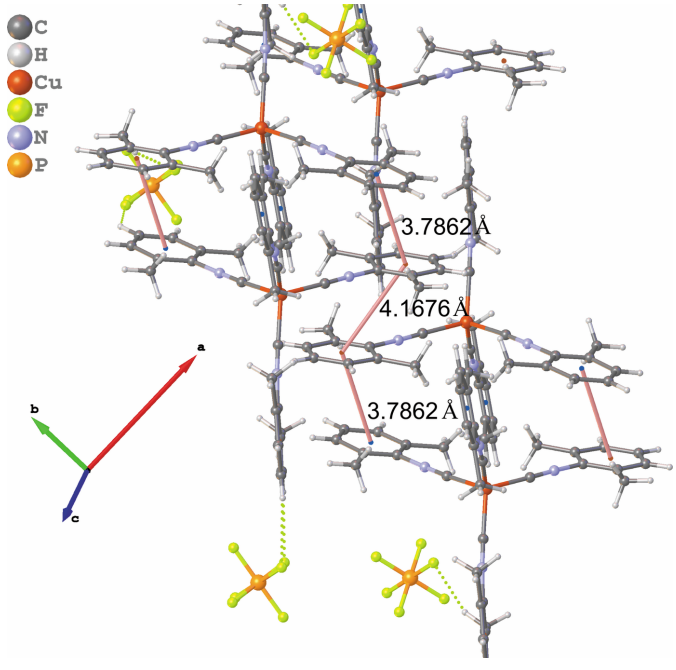

Figure 2
Supramolecular structure of $[Cu(CNXyl)_4]PF_6$ exhibiting π–π interactions (pink lines) and H···F interactions (yellow dashed lines).

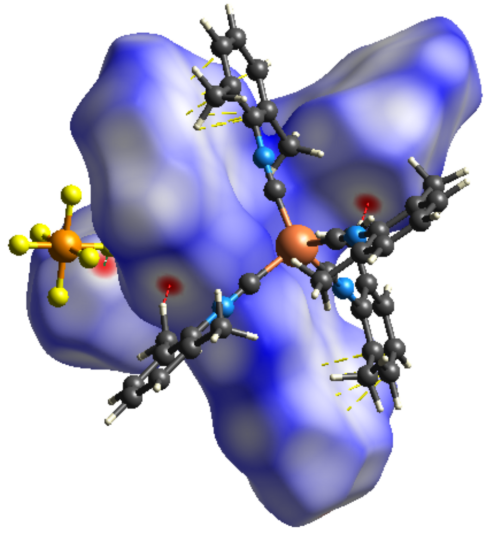

Figure 3
Hirshfeld surface of $[Cu(CNXyl)_4]PF_6$ mapped with d_{norm}. Close contacts shown are H···H (red), F···H/H···F (green), and C···C (yellow).

their aromatic rings. The angles between planes of coplanar pairs of isocyanide planes are ∼7°. This phenomenon is likely due to supramolecular interactions (*vide infra*). A similar planarity was observed for the trigonal-planar $[Cu(CNXyl)_3]^+$ (Ferraro *et al.*, 2021). All metrics associated with isocyanide ligands (C≡N bonds, CNC angles) are short and unexceptional.

3. Supramolecular features

The supramolecular structure of $[Cu(CNXyl)_4]PF_6$ (within one unit cell) is shown in Fig. 2. The drawing demonstrates a significant intermolecular interaction between neighboring complex molecules. The interaction involves offset π–π stacking, with centroid–centroid distance of 3.7862 (13) and 4.1676 (18) Å, with the latter distance being longer than expected (Janiak, 2000). Each molecule is engaged in three such interactions, forming two perpendicular chains. This interaction is likely responsible for the coplanar arrangement of two xylyl isocyanides in each complex, as it allows tighter packing. In addition, the structure demonstrates CH_3(xylyl)···PF_6 and $CHsp^2$(xylyl)···PF_6 interactions (∼2.4–2.6 Å).

4. Hirshfeld surface analysis

To quantify intermolecular interactions influencing the packing of $[Cu(CNXyl)_4]PF_6$, a Hirshfeld surface analysis was undertaken (Spackman & Jayatilaka, 2009) and the corresponding two-dimensional fingerprint plots (Spackman & McKinnon, 2002) were generated using *CrystalExplorer21.5* (Spackman *et al.*, 2021). Contacts are revealed by examining the distances from the Hirshfeld surface to the nearest atom inside the surface (d_i) and outside the surface (d_e). The d_{norm} map is the normalized contact distance using d_i and d_e normalized to the van der Waals radius. The d_{norm} map reveals contact regions that are closer than the van der Waals radii (red) to those that are longer (blue), where white is at the van der Waals radii. Fig. 3 shows H···H (red), F···H/H···F (green), and C···C (yellow) close contacts in $[Cu(CNXyl)_4]PF_6$.

The shape-index surface is useful for detecting π–π interactions, which are indicated as touching red–blue triangles (McKinnon *et al.*, 2004; Spackman & Jayatilaka, 2009). Fig. 4*a* shows a large red triangle and a large blue triangle over two xylyl rings (highlighted by red squares); however, the touching pattern appears less like triangles, but the alternating pattern and the 3.7862 Å centroid–centroid distance still indicates π–π stacking interactions (McKinnon *et al.*, 2004). Rotating the molecule by 90°, one of the xylyl rings shows a small red–blue triangle pair directly above and below the bond between two carbon atoms (Fig. 4*b* and 4*c*). The fourth xylyl ring in Fig. 4*b* does not indicate π–π interactions because a PF_6 ion is posi-

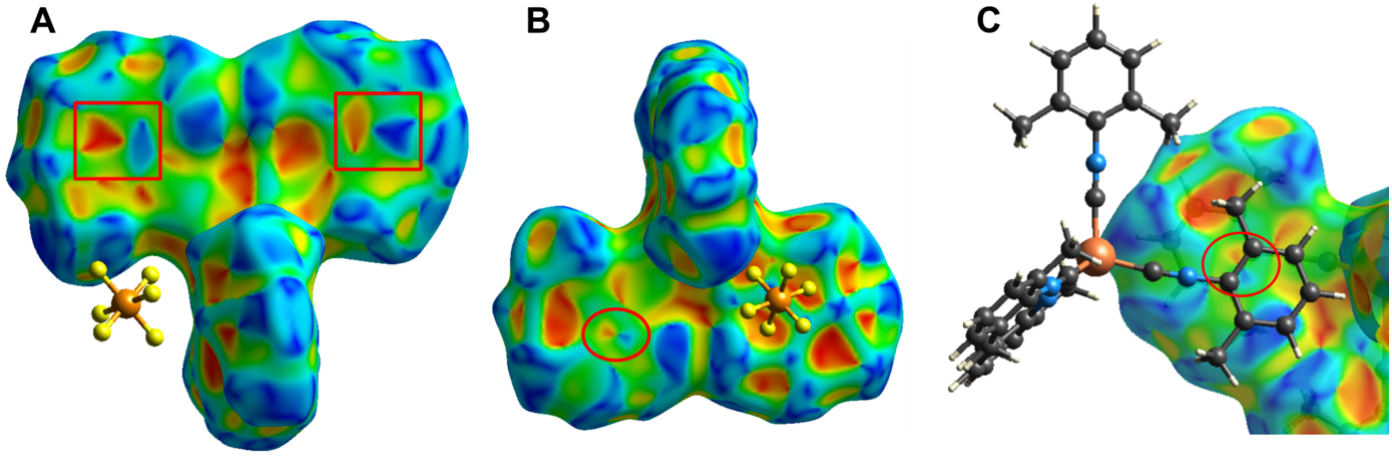

Figure 4
Hirshfeld surface mapped with shape-index. (*a*) The red squares highlight regions of large red and blue triangles over two xylyl groups (parallel to the paper). (*b*) After a 90° rotation of (*a*), there is a small red–blue triangle pair (red circle) suggesting a π–π stacking interaction. The other xylyl ring has a neighboring PF_6 ion, thus no π–π stacking interactions. (*c*) A zoomed in view of the red circle in (*b*), which shows the location of the small red–blue triangle pair aligns with the C—C bond of the two interacting xylyl rings.

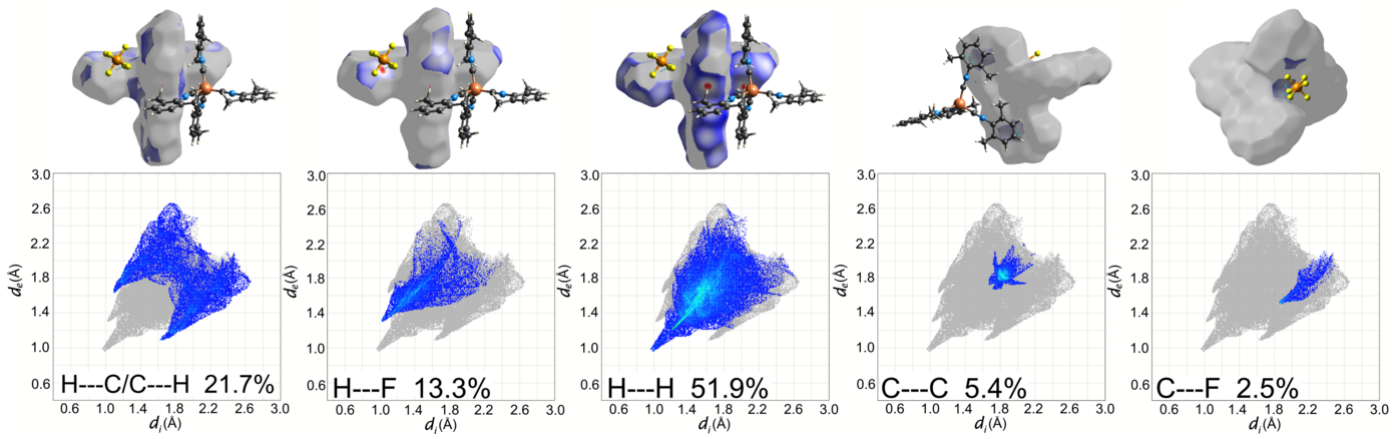

Figure 5
Fingerprint plots of $[Cu(CNXyl)_4]PF_6$ with the corresponding d_{map} interactions above the plots.

tioned above this ring. The xylyl rings in the red squares in Fig. 4*a* have a distance to the neighboring ring of 3.79 Å, which is a typical centroid–centroid distance (Janiak, 2000). The centroid–centroid distance shown in Fig. 4*c* is 4.1676 Å. Despite the unusually large centroid–centroid distance between these two xylyl rings, the shape-index surface suggests there is a π–π stacking interaction.

We can quantify each intermolecular interaction type from the two-dimensional fingerprint plots (Fig. 5), which summarize the frequency of every combination of d_e and d_i pairs, while providing specific interactions and the relative area of the interactions (McKinnon *et al.*, 2004). The majority of the short contacts are H···H (51.9%), C···H/H···C (21.7%), and F···H/H···F (13.3%), which are the intense red areas on the d_{map} (Fig. 3). The C···C interactions (π–π stacking) for $[Cu(CNXyl)_4]$ contribute 5.4%. For comparison, the tris complex, $[Cu(CNXyl)_3](BF_4)$ was also evaluated (CCDC #2073393; Ferraro *et al.*, 2021). The value of the C···C interaction was 7.8%. The smaller percentage for $[Cu(CNXyl)_4]$ may be due to the longer π–π interaction (4.166 Å), while all of the π–π planar interactions in $[Cu(CNXyl)_3]$ are ∼3.7 Å.

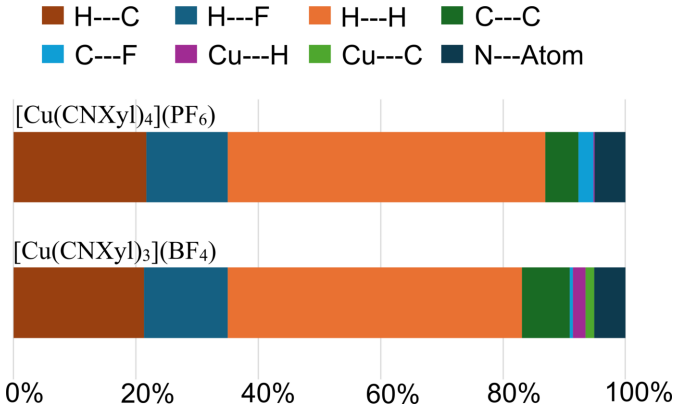

Figure 6
Percent contributions to the Hirshfeld surface area for various close intermolecular contacts for complexes $[Cu(CNXyl)_4]PF_6$ (this study) and $[Cu(CNXyl)_3](BF_4)$.

A summary of the intermolecular interactions between the tris and tetra complexes are presented in Fig. 6. In addition to the difference in C···C interactions, the other significant differences include the addition of Cu···H/H···Cu and Cu···C/C···Cu interactions for $[Cu(CNXyl)_3]$. The trigonal-planer geometry of the tris complex provides access to the Cu atom. The other difference is the larger C···F/F···C interactions for $[Cu(CNXyl)_4]PF_6$ at 2.5%, while only 0.5% for $[Cu(CNXyl)_3](BF_4)$. The additional interaction with the counter-ion for $[Cu(CNXyl)_4](PF_6)$ is likely due to the reduced C···C interactions.

5. Database survey

Looking for related structures, we conducted two database searches in the Cambridge Structural Database (WebCSD, September 2025; Groom *et al.*, 2016). The first search focused on Cu^I complexes with xylyl isocyanide. While no tetra-coordinate $[Cu(CNXyl)_4]^+$ were found, several tri-coordinate $[Cu(CNXyl)_3]^+$ were observed, as described above. We have also searched for tetra-coordinate Cu^I complexes with phenyl isocyanide; this search revealed six tetrahedral $[Cu(CNAr)_4]^+$ structures, in which CNAr was a *para*-substituted aryl isocyanide.

6. Synthesis and crystallization

$[Cu(NCMe)_4]PF_6$ (10 mg, 0.027 mmol, 1.0 equiv) was dissolved in acetonitrile (2 mL) and CNXyl [CNXyl = CN(2,6-MeC_6H_3)] (35.2 mg, 0.270 mmol, 10.0 equiv) was dissolved in acetonitrile (2 mL). Both solutions were cooled to −33 °C (238 K). The colorless solution of CNXyl was then added dropwise to a stirred colorless solution of $[Cu(NCMe)_4]PF_6$ producing a colourless solution. The reaction mixture was stirred for 1 h, after which volatiles were removed *in vacuo*. The product was obtained as a white solid (36.8 mg, 0.0502 mmol, 81%). This solid was recrystallized *via* vapor diffusion of ether into dichloromethane at 238 K to obtain colorless crystal suitable for X-ray crystallography. ^{1}H NMR

(298K, 400 MHz, CD_2Cl_2) δ 7.34 (*t*, *J* = 8 Hz, 1H), 7.22 (*d*, *J* = 8 Hz, 2H), 2.49 (*s*, 6H). ^{13}C NMR (101 MHz, CD_2Cl_2) δ 146.47 (*C*NXyl), 136.56, 131.11, 129.01, 126.09, 19.24. IR (cm^{-1}, selected peaks) 2153 (*vs*, C≡NXyl).

7. Refinement

Crystal data, data collection and structure refinement details are summarized in Table 2. The hydrogen atoms were positioned with idealized geometry and refined isotropically using a riding model.

Acknowledgements

The authors have no conflict of interest to declare.

Funding information

Funding for this research was provided by: The National Science Foundation (grant No. CHE-2348382); National Institutes of Health (grant No. 3R01EB027103-02S1).

Table 2
Experimental details.

Crystal data	
Chemical formula	$[Cu(C_9H_9N)_4]PF_6$
M_r	733.20
Crystal system, space group	Monoclinic, *C*2/*c*
Temperature (K)	100
a, *b*, *c* (Å)	25.4731 (7), 10.7452 (3), 15.1475 (4)
β (°)	121.770 (1)
V (Å^3)	3524.86 (17)
Z	4
Radiation type	Mo *K*α
μ (mm^{-1})	0.73
Crystal size (mm)	0.20 × 0.15 × 0.10
Data collection	
Diffractometer	Bruker D8 VENTURE
Absorption correction	Multi-scan (*SADABS*; Krause *et al.*, 2015)
T_{min}, T_{max}	0.724, 0.742
No. of measured, independent and observed [$I > 2\sigma(I)$] reflections	92973, 4046, 3500
R_{int}	0.052
$(\sin\theta/\lambda)_{max}$ (Å^{-1})	0.650
Refinement	
$R[F^2 > 2\sigma(F^2)]$, $wR(F^2)$, *S*	0.032, 0.101, 1.07
No. of reflections	4046
No. of parameters	223
H-atom treatment	H-atom parameters constrained
$\Delta\rho_{max}$, $\Delta\rho_{min}$ (e Å^{-3})	0.24, −0.17

Computer programs: *APEX6* and *SAINT* (Bruker, 2024), *SHELXT* (Sheldrick, 2015*a*), *SHELXL2019/3* (Sheldrick, 2015*b*) and *OLEX2* (Dolomanov *et al.*, 2009).

References

Balto, K. P., Gembicky, M., Rheingold, A. L. & Figueroa, J. S. (2021). *Inorg. Chem.* **60**, 12545–12554.
Bartholomew, A. K., Stone, I. B., Steigerwald, M. L., Lambert, T. H. & Roy, X. (2022). *J. Am. Chem. Soc.* **144**, 16773–16777.
Bell, A., Walton, R. A., Edwards, D. A. & Poulter, M. A. (1985). *Inorg. Chim. Acta* **104**, 171–178.
Bruker (2024). *APEX6* and *SAINT*. Bruker AXS Inc., Madison, Wisconsin, USA.
Chandima, A. M. B., Sgro, G., Hilditch, S. M., Kaluarachchige Don, U. I., Ward, C. L., Anderson, D. P., Herman, L., Gelman, D., Lord, R. L. & Groysman, S. (2025). *Dalton Trans.* **54**, 14716–14727.
Claude, G., Puccio, D., Roca Jungfer, M., Hagenbach, A., Spreckelmeyer, S. & Abram, U. (2023). *Inorg. Chem.* **62**, 12445–12452.
Dobbek, H., Gremer, L., Kiefersauer, R., Huber, R. & Meyer, O. (2002). *Proc. Natl Acad. Sci. USA* **99**, 15971–15976.
Dolomanov, O. V., Bourhis, L. J., Gildea, R. J., Howard, J. A. K. & Puschmann, H. (2009). *J. Appl. Cryst.* **42**, 339–341.
Ferraro, V., Sole, R. & Álvarez–Miguel, L. (2023). *Appl. Organomet. Chem.* **37**, e7182.
Ferraro, V., Sole, R., Bortoluzzi, M., Beghetto, V. & Castro, J. (2021). *Appl. Organomet. Chem.* **35**, e6401.
Fox, B. J., Sun, Q. Y., DiPasquale, A. G., Fox, A. R., Rheingold, A. L. & Figueroa, J. S. (2008). *Inorg. Chem.* **47**, 9010–9020.
Groom, C. R., Bruno, I. J., Lightfoot, M. P. & Ward, S. C. (2016). *Acta Cryst.* B**72**, 171–179.
Hollingsworth, T. S., Hollingsworth, R. L., Lord, R. L. & Groysman, S. (2018). *Dalton Trans.* **47**, 10017–10024.
Janiak, C. (2000). *J. Chem. Soc. Dalton Trans.* pp. 3885–3896.
Kaluarachchige Don, U. I., Almaat, A. S., Ward, C. L. & Groysman, S. (2023*a*). *Molecules* **28**, 3644.
Kaluarachchige Don, U. I., Chandima, A. M. B., Gelman, D., Lord, R. L. & Groysman, S. (2024). *Comments Inorg. Chem.* **44**, 349–384.
Kaluarachchige Don, U. I., Kurup, S. S., Hollingsworth, T. S., Ward, C. L., Lord, R. L. & Groysman, S. (2021). *Inorg. Chem.* **60**, 14655–14666.
Kaluarachchige Don, U. I., Palmer, Z., Ward, C. L., Lord, R. L. & Groysman, S. (2023*b*). *Inorg. Chem.* **62**, 15063–15075.
Kinzhalov, M. A., Ivanov, D. M., Melekhova, A. A., Bokach, N. A., Gomila, R. M., Frontera, A. & Kukushkin, V. Y. (2022). *Inorg. Chem. Front.* **9**, 1655–1665.
Kinzhalov, M. A., Ivanov, D. M., Shishkina, A. V., Melekhova, A. A., Suslonov, V. V., Frontera, A., Kukushkin, V. Y. & Bokach, N. A. (2023). *Inorg. Chem. Front.* **10**, 1522–1533.
Krause, L., Herbst-Irmer, R., Sheldrick, G. M. & Stalke, D. (2015). *J. Appl. Cryst.* **48**, 3–10.
McKinnon, J. J., Spackman, M. A. & Mitchell, A. S. (2004). *Acta Cryst.* B**60**, 627–668.
Melekhova, A. A., Novikov, A. S., Luzyanin, K. V., Bokach, N. A., Starova, G. L., Gurzhiy, V. V. & Kukushkin, V. Y. (2015). *Inorg. Chim. Acta* **434**, 31–36.
Perrine, C. L., Zeller, M., Woolcock, J., Styranec, T. M. & Hunter, A. D. (2010). *J. Chem. Crystallogr.* **40**, 289–295.
Ruiz, J. & Mateo, M. A. (2022). *Dalton Trans.* **51**, 13199–13203.
Sheldrick, G. M. (2015*a*). *Acta Cryst.* A**71**, 3–8.
Sheldrick, G. M. (2015*b*). *Acta Cryst.* C**71**, 3–8.
Spackman, M. A. & Jayatilaka, D. (2009). *CrystEngComm* **11**, 19–32.
Spackman, M. A. & McKinnon, J. J. (2002). *CrystEngComm* **4**, 378–392.
Spackman, P. R., Turner, M. J., McKinnon, J. J., Wolff, S. K., Grimwood, D. J., Jayatilaka, D. & Spackman, M. A. (2021). *J. Appl. Cryst.* **54**, 1006–1011.

supporting information

Acta Cryst. (2025). E**81**, 1153-1157 [https://doi.org/10.1107/S2056989025009867]

Synthesis and structure of a tetrahedral homoleptic Cu^{I} complex with xylyl isocyanide

A. M. Buddhika Chandima, Stanislav Groysman and Cassandra L. Ward

Computing details

Tetrakis(2,6-dimethylphenylisocyanide)copper(I) hexafluorophosphate

Crystal data

$[Cu(C_9H_9N)_4]PF_6$
M_r = 733.20
Monoclinic, $C2/c$
a = 25.4731 (7) Å
b = 10.7452 (3) Å
c = 15.1475 (4) Å
β = 121.770 (1)°
V = 3524.86 (17) Å^3
Z = 4
$F(000)$ = 1512
D_x = 1.382 Mg m^{-3}
Mo $K\alpha$ radiation, λ = 0.71073 Å
Cell parameters from 9948 reflections
θ = 2.3–27.0°
μ = 0.73 mm^{-1}
T = 100 K
Prism, colourless
0.2 × 0.15 × 0.1 mm

Data collection

Bruker D8 VENTURE diffractometer
Radiation source: microfocus sealed tube, Incoatec IμS
Multilayer mirror monochromator
φ and ω scans
Absorption correction: multi-scan (SADABS; Krause *et al.*, 2015)
T_{min} = 0.724, T_{max} = 0.742
92973 measured reflections
4046 independent reflections
3500 reflections with $I > 2\sigma(I)$
R_{int} = 0.052
θ_{max} = 27.5°, θ_{min} = 2.1°
h = −33→33
k = −13→13
l = −19→19

Refinement

Refinement on F^2
Least-squares matrix: full
$R[F^2 > 2\sigma(F^2)]$ = 0.032
$wR(F^2)$ = 0.101
S = 1.07
4046 reflections
223 parameters
0 restraints
Hydrogen site location: inferred from neighbouring sites
H-atom parameters constrained
$w = 1/[\sigma^2(F_o^2) + (0.0527P)^2 + 1.8864P]$ where $P = (F_o^2 + 2F_c^2)/3$
$(\Delta/\sigma)_{max}$ = 0.001
$\Delta\rho_{max}$ = 0.24 e Å^{-3}
$\Delta\rho_{min}$ = −0.17 e Å^{-3}

Special details

Experimental. A suitable crystal was mounted on a Bruker D8 Venture diffractometer with kappa geometry, an Incoatec IμS micro-focus source X-ray tube (Mo K_α radiation), and a multilayer mirror for monochromatization. The diffraction intensities were measured using a Photon III CPAD area detector. Data were acquired at 100 K with an Oxford 800 Cryostream low-temperature apparatus. Using APEX6 v2024.9-0, the intensities were integrated using SAINT V8.40b and a multiscan absorption correction was applied with SADABS-2016/2. The crystal structure was solved and refined using SHELXT (Sheldrick, 2015a) and least-squares refinement with SHELXL-2019/3 (Sheldrick, 2015b) running under Olex2 (Dolomanov *et al.*, 2009). All non–hydrogen atoms were refined anisotropically.

Geometry. All esds (except the esd in the dihedral angle between two l.s. planes) are estimated using the full covariance matrix. The cell esds are taken into account individually in the estimation of esds in distances, angles and torsion angles; correlations between esds in cell parameters are only used when they are defined by crystal symmetry. An approximate (isotropic) treatment of cell esds is used for estimating esds involving l.s. planes.

Refinement. The 200 and 111 reflections were omitted due to being blocked or partially blocked by the beam stop. The other three reflections were omitted for large Fcalc. Non-merohedral and pseudo-merohedral twinning was looked for but did not find a suitable twin law or a second domain.

Fractional atomic coordinates and isotropic or equivalent isotropic displacement parameters (Å²)

	x	*y*	*z*	U_{iso}*/U_{eq}
Cu1	0.500000	0.33279 (3)	0.250000	0.04408 (11)
P1	0.250000	0.750000	0.500000	0.0623 (2)
F1	0.24423 (7)	0.60646 (15)	0.51955 (11)	0.0860 (4)
F2	0.18029 (6)	0.74986 (16)	0.40429 (10)	0.0844 (4)
F3	0.27340 (7)	0.71339 (17)	0.42396 (10)	0.0837 (4)
N1	0.44524 (7)	0.17581 (14)	0.35511 (12)	0.0524 (4)
N2	0.40387 (7)	0.49851 (15)	0.06716 (11)	0.0532 (4)
C1	0.46296 (8)	0.23207 (18)	0.31124 (13)	0.0507 (4)
C2	0.43813 (8)	0.43636 (19)	0.13574 (13)	0.0527 (4)
C3	0.42734 (9)	0.10442 (18)	0.41253 (15)	0.0532 (4)
C4	0.45639 (9)	0.1277 (2)	0.51896 (16)	0.0615 (5)
C5	0.43930 (11)	0.0512 (3)	0.57417 (18)	0.0756 (7)
H5	0.461572	0.064477	0.658697	0.091*
C6	0.39537 (12)	−0.0403 (2)	0.5258 (2)	0.0799 (7)
H6	0.383238	−0.099785	0.571846	0.096*
C7	0.36633 (12)	−0.0582 (2)	0.4197 (2)	0.0742 (6)
H7	0.330330	−0.130185	0.381418	0.089*
C8	0.38227 (11)	0.01436 (19)	0.36079 (17)	0.0618 (5)
C9	0.35095 (14)	−0.0037 (3)	0.2452 (2)	0.0835 (7)
H9A	0.384325	−0.040329	0.226918	0.125*
H9B	0.333033	0.085889	0.205852	0.125*
H9C	0.312661	−0.069704	0.218740	0.125*
C10	0.50276 (10)	0.2294 (3)	0.56955 (18)	0.0797 (7)
H10A	0.538384	0.211912	0.563170	0.119*
H10B	0.516293	0.234284	0.643171	0.119*
H10C	0.484074	0.308693	0.535562	0.119*
C11	0.36347 (8)	0.57934 (18)	−0.01298 (12)	0.0493 (4)
C12	0.33917 (9)	0.6776 (2)	0.01145 (16)	0.0580 (5)
C13	0.30131 (10)	0.7600 (2)	−0.0679 (2)	0.0714 (6)
H13	0.281228	0.840924	−0.051329	0.086*

C14	0.28884 (10)	0.7408 (2)	−0.16689 (19)	0.0748 (7)
H14	0.258547	0.806384	−0.229230	0.090*
C15	0.31333 (11)	0.6422 (3)	−0.18888 (16)	0.0768 (7)
H15	0.302400	0.628829	−0.269041	0.092*
C16	0.35194 (10)	0.5577 (2)	−0.11239 (14)	0.0643 (5)
C17	0.35335 (15)	0.6937 (3)	0.1207 (2)	0.0968 (9)
H17A	0.342084	0.617649	0.142587	0.145*
H17B	0.329636	0.763969	0.123090	0.145*
H17C	0.397576	0.709823	0.167384	0.145*
C18	0.38040 (17)	0.4495 (4)	−0.1342 (2)	0.1130 (12)
H18A	0.367041	0.362761	−0.112933	0.169*
H18B	0.430846	0.458695	−0.088595	0.169*
H18C	0.364182	0.447586	−0.217197	0.169*

Atomic displacement parameters (Å²)

	U^{11}	U^{22}	U^{33}	U^{12}	U^{13}	U^{23}
Cu1	0.04500 (17)	0.0608 (2)	0.02891 (14)	0.000	0.02116 (12)	0.000
P1	0.0586 (4)	0.0893 (6)	0.0406 (3)	0.0024 (4)	0.0273 (3)	0.0124 (3)
F1	0.0929 (10)	0.0894 (10)	0.0810 (9)	0.0009 (8)	0.0494 (8)	0.0180 (8)
F2	0.0618 (7)	0.1242 (12)	0.0539 (7)	0.0025 (7)	0.0212 (6)	0.0119 (7)
F3	0.0869 (9)	0.1199 (11)	0.0611 (7)	0.0040 (8)	0.0505 (7)	0.0068 (8)
N1	0.0543 (8)	0.0602 (9)	0.0554 (9)	0.0128 (7)	0.0376 (7)	0.0126 (7)
N2	0.0500 (8)	0.0657 (9)	0.0377 (7)	−0.0025 (7)	0.0189 (6)	0.0055 (7)
C1	0.0496 (9)	0.0642 (11)	0.0448 (9)	0.0087 (8)	0.0294 (8)	0.0075 (8)
C2	0.0517 (9)	0.0687 (11)	0.0362 (8)	−0.0021 (8)	0.0222 (7)	0.0021 (8)
C3	0.0597 (10)	0.0593 (10)	0.0600 (10)	0.0180 (8)	0.0449 (9)	0.0184 (8)
C4	0.0512 (10)	0.0862 (14)	0.0564 (10)	0.0201 (10)	0.0348 (9)	0.0187 (10)
C5	0.0691 (13)	0.1117 (19)	0.0617 (12)	0.0289 (13)	0.0453 (11)	0.0335 (13)
C6	0.0910 (16)	0.0878 (16)	0.0933 (17)	0.0238 (14)	0.0709 (15)	0.0371 (14)
C7	0.0938 (16)	0.0618 (12)	0.1006 (18)	0.0089 (11)	0.0742 (15)	0.0136 (12)
C8	0.0822 (13)	0.0541 (10)	0.0757 (13)	0.0104 (9)	0.0598 (12)	0.0070 (9)
C9	0.115 (2)	0.0801 (15)	0.0827 (16)	−0.0166 (14)	0.0705 (16)	−0.0189 (13)
C10	0.0522 (11)	0.122 (2)	0.0613 (13)	0.0046 (12)	0.0275 (10)	0.0032 (13)
C11	0.0442 (8)	0.0626 (10)	0.0353 (7)	−0.0056 (7)	0.0169 (7)	0.0067 (7)
C12	0.0475 (9)	0.0738 (13)	0.0513 (10)	−0.0034 (8)	0.0250 (8)	0.0017 (9)
C13	0.0499 (10)	0.0734 (14)	0.0846 (16)	0.0029 (9)	0.0310 (11)	0.0117 (11)
C14	0.0505 (11)	0.0899 (16)	0.0669 (13)	−0.0002 (11)	0.0191 (10)	0.0337 (12)
C15	0.0661 (13)	0.1111 (19)	0.0409 (10)	−0.0056 (13)	0.0198 (9)	0.0199 (11)
C16	0.0625 (11)	0.0851 (14)	0.0382 (9)	−0.0007 (10)	0.0216 (8)	0.0016 (9)
C17	0.0942 (19)	0.136 (3)	0.0633 (15)	0.0190 (17)	0.0438 (14)	−0.0132 (15)
C18	0.136 (3)	0.134 (3)	0.0610 (15)	0.033 (2)	0.0463 (17)	−0.0132 (16)

Geometric parameters (Å, º)

Cu1—C1	1.9605 (18)	C8—C9	1.506 (3)
Cu1—C1^{i}	1.9606 (18)	C9—H9A	1.0970
Cu1—C2	1.9610 (18)	C9—H9B	1.0970

Cu1—C2^{i}	1.9610 (18)	C9—H9C	1.0970
P1—F1^{ii}	1.5919 (15)	C10—H10A	0.9800
P1—F1	1.5919 (15)	C10—H10B	0.9800
P1—F2	1.5950 (13)	C10—H10C	0.9800
P1—F2^{ii}	1.5951 (13)	C11—C12	1.370 (3)
P1—F3^{ii}	1.5998 (13)	C11—C16	1.393 (3)
P1—F3	1.5999 (13)	C12—C13	1.392 (3)
N1—C1	1.152 (2)	C12—C17	1.506 (3)
N1—C3	1.404 (2)	C13—H13	1.1030
N2—C2	1.154 (2)	C13—C14	1.375 (4)
N2—C11	1.404 (2)	C14—H14	1.1030
C3—C4	1.397 (3)	C14—C15	1.357 (4)
C3—C8	1.386 (3)	C15—H15	1.1030
C4—C5	1.395 (3)	C15—C16	1.391 (3)
C4—C10	1.491 (4)	C16—C18	1.497 (4)
C5—H5	1.1030	C17—H17A	0.9800
C5—C6	1.376 (4)	C17—H17B	0.9800
C6—H6	1.1030	C17—H17C	0.9800
C6—C7	1.384 (4)	C18—H18A	1.0970
C7—H7	1.1030	C18—H18B	1.0970
C7—C8	1.397 (3)	C18—H18C	1.0970

C1—Cu1—C1^{i}	112.99 (11)	C8—C9—H9A	109.5
C1^{i}—Cu1—C2^{i}	111.56 (7)	C8—C9—H9B	109.5
C1—Cu1—C2	111.56 (7)	C8—C9—H9C	109.5
C1—Cu1—C2^{i}	105.02 (8)	H9A—C9—H9B	109.5
C1^{i}—Cu1—C2	105.01 (8)	H9A—C9—H9C	109.5
C2^{i}—Cu1—C2	110.85 (11)	H9B—C9—H9C	109.5
F1—P1—F1^{ii}	180.0	C4—C10—H10A	109.5
F1^{ii}—P1—F2^{ii}	90.03 (8)	C4—C10—H10B	109.5
F1^{ii}—P1—F2	89.97 (8)	C4—C10—H10C	109.5
F1—P1—F2	90.03 (8)	H10A—C10—H10B	109.5
F1—P1—F2^{ii}	89.97 (8)	H10A—C10—H10C	109.5
F1—P1—F3^{ii}	89.91 (8)	H10B—C10—H10C	109.5
F1^{ii}—P1—F3	89.90 (8)	C12—C11—N2	118.23 (16)
F1—P1—F3	90.09 (8)	C12—C11—C16	123.53 (18)
F1^{ii}—P1—F3^{ii}	90.10 (8)	C16—C11—N2	118.21 (18)
F2—P1—F2^{ii}	180.0	C11—C12—C13	117.58 (19)
F2^{ii}—P1—F3	89.78 (8)	C11—C12—C17	120.2 (2)
F2—P1—F3	90.22 (8)	C13—C12—C17	122.2 (2)
F2—P1—F3^{ii}	89.78 (8)	C12—C13—H13	119.9
F2^{ii}—P1—F3^{ii}	90.22 (8)	C14—C13—C12	120.2 (2)
F3^{ii}—P1—F3	180.0	C14—C13—H13	119.9
C1—N1—C3	176.48 (18)	C13—C14—H14	119.6
C2—N2—C11	177.1 (2)	C15—C14—C13	120.8 (2)
N1—C1—Cu1	174.35 (17)	C15—C14—H14	119.6
N2—C2—Cu1	176.58 (16)	C14—C15—H15	119.3
C4—C3—N1	118.02 (19)	C14—C15—C16	121.3 (2)

C8—C3—N1	118.27 (17)	C16—C15—H15	119.3
C8—C3—C4	123.71 (18)	C11—C16—C18	121.2 (2)
C3—C4—C10	121.26 (19)	C15—C16—C11	116.5 (2)
C5—C4—C3	116.3 (2)	C15—C16—C18	122.4 (2)
C5—C4—C10	122.4 (2)	C12—C17—H17A	109.5
C4—C5—H5	119.2	C12—C17—H17B	109.5
C6—C5—C4	121.6 (2)	C12—C17—H17C	109.5
C6—C5—H5	119.2	H17A—C17—H17B	109.5
C5—C6—H6	119.8	H17A—C17—H17C	109.5
C5—C6—C7	120.3 (2)	H17B—C17—H17C	109.5
C7—C6—H6	119.8	C16—C18—H18A	109.5
C6—C7—H7	119.7	C16—C18—H18B	109.5
C6—C7—C8	120.5 (2)	C16—C18—H18C	109.5
C8—C7—H7	119.7	H18A—C18—H18B	109.5
C3—C8—C7	117.4 (2)	H18A—C18—H18C	109.5
C3—C8—C9	121.42 (19)	H18B—C18—H18C	109.5
C7—C8—C9	121.1 (2)		

N1—C3—C4—C5	−177.29 (17)	C6—C7—C8—C9	−179.8 (2)
N1—C3—C4—C10	3.0 (3)	C8—C3—C4—C5	2.2 (3)
N1—C3—C8—C7	178.19 (17)	C8—C3—C4—C10	−177.48 (19)
N1—C3—C8—C9	−2.6 (3)	C10—C4—C5—C6	178.5 (2)
N2—C11—C12—C13	177.32 (17)	C11—C12—C13—C14	0.7 (3)
N2—C11—C12—C17	−3.0 (3)	C12—C11—C16—C15	−0.2 (3)
N2—C11—C16—C15	−177.91 (18)	C12—C11—C16—C18	179.3 (3)
N2—C11—C16—C18	1.6 (3)	C12—C13—C14—C15	−0.4 (3)
C3—C4—C5—C6	−1.2 (3)	C13—C14—C15—C16	−0.3 (4)
C4—C3—C8—C7	−1.3 (3)	C14—C15—C16—C11	0.5 (3)
C4—C3—C8—C9	177.9 (2)	C14—C15—C16—C18	−178.9 (3)
C4—C5—C6—C7	−0.6 (4)	C16—C11—C12—C13	−0.4 (3)
C5—C6—C7—C8	1.6 (4)	C16—C11—C12—C17	179.3 (2)
C6—C7—C8—C3	−0.6 (3)	C17—C12—C13—C14	−179.0 (2)

Symmetry codes: (i) −*x*+1, *y*, −*z*+1/2; (ii) −*x*+1/2, −*y*+3/2, −*z*+1.